ARTICLES

A Novel Synthetic Peptide Polymer with Cyclic RGD Motifs Supports Serum-Free Attachment of Anchorage-Dependent Cells

K. Markó,*[,†,‡] M. Ligeti,[†,§] G. Mező,[§] N. Mihala,[§] E. Kutnyánszky,[||] É. Kiss,[||] F. Hudecz,[§,⊥] and E. Madarász[‡]

Institute of Experimental Medicine, Hungarian Academy of Sciences, Szigony u. 43. 1083, Budapest, Research Group of Peptide Chemistry, Hungarian Academy of Sciences; Laboratory of Interfaces and Nanostructures, Institute of Chemistry; and Department of Organic Chemistry, Eötvös Loránd University, P.O. Box 32, Budapest 112 H-1518, Hungary. Received January 10, 2008; Revised Manuscript Received June 21, 2008

Cell adhesivity is a basic biological principle, which provides mechanisms for construction of multicellular organisms, tissue genesis, migration and individual cell survival. *In vivo*, the cell adhesive environment is provided by extracellular matrix molecules, neighboring cell surfaces and soluble factors delivered either by tissue cells or by blood circulation. The exact molecular composition of the microenvironment of a cell is not properly understood. The nondefined molecular composition of "native" adhesive components hinders their application when defined culture conditions are necessary, as, for an example, growing human cells for further clinical application. Applying large, substrate-coating molecules as backbones for carrying specific adhesive peptide motifs provides a relatively cheap, reproducible, and chemically defined group of synthetic adhesion molecules. Here, we report on the design, synthesis, and testing of a novel cyclic RGD-containing coating material, which promotes initial attachment, spreading, survival, and proliferation of a number of different cell types. The potent adhesive polypeptide-brush, composed of poly[Lys(DL-Ala_m)] branched chain polypeptide (AK) and multiple copies of cyclic(arginyl-glycyl-aspartyl-D-phenylalanyl-cysteine) pentapeptide prevents anoikis and supports cell attachment in the absence of serum or other biological additives. The defined conditions for cell maintenance make this material a promising candidate for coating artificial cell substrates even for therapeutic applications.

1. INTRODUCTION

Cell−extracellular matrix (ECM) interactions are pivotal for survival of adherent cells both *in vivo* and *in vitro*. Without proper attachment, cells adopt a special apoptotic fate, termed "anoikis" (homelessness in Greek) (*1*). For *in vitro* maintenance of adherent cells, artificial substrates should provide appropriate surfaces for rapid attachment.

In traditional cell culture techniques, sera of various origins, containing different attachment and spreading factors, are included in the culture medium. While serum application greatly helps cell culturing, its nondefined nature makes it ineligible when defined culture conditions are required, such as for growing human cells for clinical applications. Its high price, the risk of contamination, and the animal welfare considerations also hinder the use of sera (*2*).

Serum-free, chemically defined media are available for a wide variety of cell types (*3*), but most of them impair cell attachment. Coating the culture surfaces with native extracellular matrix molecules derived from either human/animal tissues or recombinant bacteria may overcome this difficulty but brings back the uncertainty in molecular composition and the risk of contamination. Synthetic, polycationic peptides/proteins, such as poly(L/D-lysine) (PLL, PDL) or polyornithine, are widely used for coating cell culture dishes. Such nonspecific adhesive coatings, however, promote initial cell adhesion with moderate efficiency, may cause abnormal cell-spreading, and might be cytotoxic (*4*). Applying such large, substrate-coating molecules as backbones for carrying specific adhesive peptide motifs, however, may provide a relatively cheap, reproducible, and chemically defined group of efficient synthetic adhesion molecules (*5*).

Cell−ECM adhesion is performed predominantly by integrins which serve as receptors for several ECM components (*6*). Besides anchoring the cells, signaling through the integrins can regulate the survival, proliferation, and differentiation of cells (*7*).

Various scaffold substrates had been modified with RGD motifs (*5, 8*−*16*), a tripeptide sequence recognized by most integrins. The RGD (arginyl-glycyl-aspartic acid) sequence can be found in many extracellular matrix proteins (fibronectin, vitronectin, tenascin-C, etc.) and is responsible for the binding of these ECM proteins to their receptors (*17*) on the cell surfaces. In soluble form, RGD-containing oligopeptides can inhibit cell adhesion, by antagonizing the integrin−matrix interaction (*18*). The immobilized RGD sequence, on the other hand, is generally acknowledged as a promising biomaterial for promoting cell adhesion to artificial substrates and it is the most commonly

* Corresponding author. E-mail: marko@koki.hu. Fax: 36 1 2109966. Address: Szigony u. 43. 1083, Budapest, Hungary.

† These authors contributed equally to this work.

‡ Institute of Experimental Medicine, Hungarian Academy of Sciences.

§ Research Group of Peptide Chemistry, Hungarian Academy of Sciences, Eötvös Loránd University.

|| Laboratory of Interfaces and Nanostructures, Institute of Chemistry, Eötvös Loránd University.

⊥ Department of Organic Chemistry, Eötvös Loránd University.

10.1021/bc8000134 CCC: $40.75
Published on Web 08/13/2008

applied protein motif on synthetic surfaces (*5*). Because of the uncovered carboxyl terminus of the aspartate residue, the RGD tripeptide, in itself, has no biological activity. In the active RGD motif, this C-terminus should be masked by addition of another amino acid (*18*). RGD-containing cyclic pentapeptides, such as cyclo[RGDfV], were originally described as potent inhibitors of cell adhesion to vitronectin and laminin fragment P1 (*19*). Cyclic (RGDfV) (*20*), (RGDfK) (*21*), and (RGDfC) peptides have the highest affinity and selectivity toward $\alpha_v\beta_3$ and bind strongly to $\alpha_v\beta_5$, $\alpha_v\beta_6$ (*22*) integrins and with lower affinity to other integrins (such as $\alpha_{IIb}\beta_3$ and $\alpha_5\beta_1$), as well (*20*).

In order to obtain an integrin-binding macromolecule, we designed a poly[Lys(DL-Ala_m)] (AK) branched polypeptide, carrying multiple copies of cyclic(arginyl-glycyl-aspartyl-D-phenylalanyl-cysteine) pentapeptide on the N-terminal positions of the oligoalanine branches (AK-cyclo[RGDfC]). The novel synthetic polypeptide readily adsorbed to various solid substrates and provided a strongly adhesive coating for cell attachment. In order to evaluate selective versus general adhesiveness of the polymer, the attachment of a number of different anchorage-dependent cells was investigated. AK-cyclo[RGDfC]-coated surfaces promoted adhesion and spreading of almost all investigated cell types in the absence of serum or any other adhesion or spreading factors. As AK-cyclo[RGDfC]-coating supported serum-free survival of several cell types in the critical, 24−48 h initial attachment period, it has been proven to be a tool for initiating cell cultures under strictly defined conditions.

2. EXPERIMENTAL PROCEDURES

2.1. Materials. All amino acid derivatives and Rink-Amide MBHA resin were purchased from Novabiochem (Läufelfingen, Switzerland). Scavengers, coupling agents, and cleavage reagents were Fluka products (Buchs, Switzerland). Solvents for synthesis and 2-Cl-trityl chloride resin were obtained from Reanal (Budapest, Hungary). Acetonitrile for HPLC was delivered by Sigma-Aldrich (Budapest, Hungary).

Cell culture media and chemicals for cell culturing were purchased from Sigma-Aldrich (Budapest, Hungary). Fetal calf serum (FCS; Gibco) was purchased from Csertex (Budapest, Hungary). Tissue culture plates and dishes were Greiner or Falcon, purchased from Dialab (Budapest, Hungary) and Softflow (Pécs, Hungary), respectively, and the glass coverslips were obtained from Erie Scientific (Budaörs, Hungary).

2.2. Synthesis of Cyclo[Arg-X-Asp-D-Phe-Cys]. Linear side chain protected precursor peptides H-Asp(O^{t}Bu)-D-Phe-Cys(Trt)-Arg(Pbf)-X-OH (where X is Gly or Ala) were synthesized manually by solid-phase peptide synthetic method according to Fmoc/^{t}Bu strategy using 2-Cl-trityl chloride resin as a support (*23*). The attachment of the C-terminal amino acid to the resin was carried out as follows: (i) prior to use, the resin was dried overnight over solid KOH in a desiccator; (ii) swelling of the resin in dichloromethane (DCM) for half an hour, then washing with *N,N*-dimethylformamide (DMF); (iii) coupling of the C-terminal amino acid to the resin using 2.5 equiv of Fmoc-Gly-OH or Fmoc-Ala-OH dissolved in DMF and 2.5 equiv of *N*-ethyldiisopropylamine (DIEA) (1 + 1.5 equiv added in two portions) for 1 h, then capping with methanol (0.8 mL/g resin) for 10 min; (iv) washing with DMF (5 × 0.5 min); (v) removal of Fmoc protecting group in three steps: 5% piperidine in DMF for 10 min, 30% piperidine in DMF for 15 min, 50% piperidine in DMF for 30 min; (vi) DMF washing (6 × 1 min). The Fmoc resin loading was determined by Gude's method and resulted in 0.6 mmol/g resin capacity in both cases (*24*).

After this procedure, the further amino acid derivatives were coupled according to the following protocol: (i) coupling of Fmoc-amino acid derivative with 1-hydroxybenzotriazole (HOBt) and *N,N*′-diisopropylcarbodiimide (DIC) (3 equiv each) in DMF (the efficacy of the coupling reaction was monitored by ninhydrin assay (*25*)); (ii) DMF washing (5 × 0.5 min); (iii) deprotection in two steps with 30% piperidine in DMF for 3 and 17 min; (iv) DMF washing (6 × 1 min). After washing the peptide-resins with DMF, DCM, methanol, and diethyl ether, the side chain protected peptides were cleaved from the dried resins using a mixture of DCM/methanol/acetic acid = 8:1:1 (v/v/v) for 2 h at room temperature. The cleavage step was repeated, then the cleavage mixtures were combined and the solution was concentrated *in vacuo.* The intermediate crude product was precipitated with cold diethyl ether, filtered, and washed three times with ether afterward. The solid material was dissolved in 5% acetic acid prior to freeze-drying. The purification of the linear side chain protected peptides was not necessary due to their high purity determined by RP-HPLC (over 90%). To change the acetate counterion to chloride, the linear peptide derivatives were dissolved in methanol in the presence of 10 equiv of pyridinium hydrochloride and then the solvent was evaporated.

The dried linear peptides were dissolved in DMF (1 mg/mL), then 3−3 equiv of (benzotriazol-1-yloxy)tris(dimethylamino)-phosphonium hexafluorophosphate (BOP) and HOBt coupling agents in the presence of 6 equiv of DIEA were added to both peptide solutions. The pH of the reaction mixtures was slightly alkaline (pH 7.5−8). Each reaction was followed by RP-HPLC. After 24 h, the reactions were completed; then, the solvent was evaporated *in vacuo*, and the crude products were precipitated with 5% $NaHCO_3$ (aqueous solution), filtered off, and washed with d.i. water until the filtrate was neutral. The cleavage of the side chain protecting groups of the dried cyclic peptides was performed by using modified Reagent-K cleavage mixture: trifluoroacetic acid (9.75 mL), water (0.25 mL), phenol (0.75 g), thioanisole (0.25 mL), ethane-1,2-dithiol (0.25 mL), and triisopropyl silane (0.125 mL) at room temperature for 3.5 h. After cleavage, the crude products were precipitated with cold diethyl ether, washed with ether three times, filtered off, and dried *in vacuo* over P_2O_5, followed by purification using semipreparative RP-HPLC. The pure cyclic peptides were characterized by analytical RP-HPLC and ESI-MS (Table 1). The racemization of Ala-containing peptide under cyclization conditions was determined by using Marfey's reagent (*26, 27*). The D-Ala content of the cyclic peptide was less than 1%.

Table 1. Characteristics of Derivatives

peptides	R_T [min][a]	calculated mass [M]	$[M + H]^{+b}$
cyclo[Arg-Gly-Asp-D-Phe-Cys]	9.0	578.2	578.9
cyclo[Arg-Ala-Asp-D-Phe-Cys]	9.6	592.2	593.0
cyclo[Arg-Gly-Asp-D-Phe-Cys(Cmc)]	7.7	635.3	636.0
H-Arg-Gly-Asp-D-Phe-Cys-NH_2	6.5	595.3	596.2

[a] Column, Vydac 218TP C_{18} (250 × 4.6 mm, 5 μm, 300 Å); eluents, 0.045% TFA/H_2O (A) and 0.036% TFA/acetonitrile (B); gradient, 5−95% B in 30 min; flow rate, 1 mL/min; detection λ = 220 nm. [b] ESI-MS

2.3. Preparation of Cyclo[Arg-Gly-Asp-D-Phe-Cys(Cmc)]. The carboxamidation of the thiol group of the cyclic peptide was carried out as follows: 1 equiv of iodoacetamide to the cyclic peptide was dissolved in 0.1 M Tris buffer (pH 8.1) and the cyclic peptide was added to the solution at a peptide concentration of 1 mg/mL. The reaction was monitored by RP-HPLC. In half an hour, the reaction was completed, the mixture was acidified by addition of a few drops of TFA, and then it was purified by semipreparative RP-HPLC. Pooled fractions were freeze-dried and the purified product was characterized by analytical RP-HPLC and ESI-MS (Table 1).

2.4. Synthesis of H-Arg-Gly-Asp-D-Phe-Cys-OH. In the case of synthesis of the linear RGD peptide, it was cleaved from the 2-ClTrt resin directly by modified Reagent-K mixture and

Table 2. Amino Acid Composition of Conjugates

conjugate	Asp	Gly	Ala	Phe	Lys	Arg
AK-cyclo[RGDfC]	0.33	0.34	4.64	0.34	1.00	0.31
AK-cyclo[RADfC]	0.32	-	5.00	0.33	1.00	0.32
AK-RGDfC	0.34	0.35	4.62	0.33	1.00	0.32

the pure linear peptide was isolated by RP-HPLC purification followed by lyophilization. The purified product was characterized by analytical RP-HPLC and ESI-MS, similarly to the cyclic versions (Table 1).

2.5. Conjugation of Peptides to Chloroacetylated Branched Chain Polymeric Polypeptide. Branched chain polymeric polypeptide (poly[Lys(DL-Ala_m)]; AK) was prepared according to the method previously described (*28*). Chloroacetylation of AK polymer was performed as described before (*29*). Briefly, for the preparation of conjugate, AK ($DP_n = 60$, Ala/Lys= 4.6: 1, $M_w = 19\,600$) was reacted with chloroacetic acid pentachlorophenyl ester in DMF/water solution (9/1, v/v): first, 20 mg AK was dissolved in 1 mL water, and then the solution was diluted with 4 mL DMF; after that, 0.5 equiv chloroacetic acid pentachlorophenyl ester (ClAc-OPcp) calculated to the branches (8.2 mg) dissolved in 5 mL DMF was added. The reaction was carried out overnight, and then the mixture was dialyzed against 1% acetic acid for two days. The precipitate (pentachlorophenol) was filtered off and the filtrate was freeze-dried. According to the organic chlorine determination, the molar ratio of chlorine and lysine in polypeptide was 0.4:1 (*30*).

The conjugation reaction of multivalent chloroacetyl-AK polymer and cyclo[RXDfC] peptides or linear H-RGDfC-NH_2 peptide resulting in a thioether linkage was carried out in 0.1 M Tris buffer, pH 8.0. To avoid significant dimerization of RGD peptide derivatives *via* disulfide bond formation, the cysteine containing peptides (2 equiv altogether to the Cl content of the polymer) were added in solid form to the solution of the chloroacetylated polypeptide (1 mg/mL) from time to time during 3 h. In all cases, the reaction was terminated after 24 h by adding an excess of cysteine to block the unreacted chloroacetyl groups. The crude products were dialyzed against d.i. water to remove the unreacted RGD peptides and cyst(e)ine, then freeze-dried. The efficacy of the conjugation was calculated from the amino acid composition of the conjugates using amino acid analysis (Table 2).

2.6. Analysis and Purification by RP-HPLC. Analytical RP-HPLC measurements for the determination of the purity of intermediate peptide derivatives (for cyclization or conjugation) were carried out on Vydac 218TP C_{18} column, 250 × 4.6 mm, particle size 5 μm, pore size 300 Å (Vydac, Hesperia, CA) using Shimadzu HPLC system (two LC-6A pump, SPD-6AV UV-detector, SIL-6B auto injector, SCL-6B system controller; (Shimadzu Corporation, Kyoto, Japan)) with eluent A: 0.045% TFA in H_2O and eluent B: 0.036% TFA in acetonitrile. Linear gradient of 5−95% eluent B was developed with 1 mL/min flow rate, during 30 min. Peaks were detected at $\lambda = 220$ nm.

Purification of peptides was performed using Phenomenex Jupiter C_{18} column (250 × 10 mm, 10 μm, 300 Å) on a Knauer laboratory assembled semipreparative HPLC system (Knauer Pump type 120, Dynamic Mixing Chamber Analytical, Spectro Photometer K-2501; (Knauer, Berlin, Germany)); with eluent A: 0.1% TFA in H_2O and eluent B: 0.1% TFA in acetonitrile−H_2O (80:20, v/v). An isocratic elution with 10% of eluent B was applied from 0 to 5 min, then 5−28 min a gradient elution of 10−33% of eluent B was used with 4 mL/min flow rate. Peaks were detected at $\lambda = 220$ nm.

2.7. ESI Mass Spectrometry Analysis. The identification of the products was achieved by mass spectrometry. Electrospray ionization mass spectrometry was performed with a Bruker Daltonics Esquire 3000 Plus (Bremen, Germany) ion trap mass spectrometer, operating in continuous sample injection at 4 μL/min flow rate. The peptides were dissolved in 50% acetonitrile−water mixture. Mass spectra were recorded in positive ion mode in the m/z 200−1500 range.

2.8. Amino Acid Analysis. The amino acid composition of conjugates was determined by amino acid analysis using SYKAM S-433 amino acid analyzer (SYKAM GmbH, Eresing, Germany) equipped for the determination of amino acids with postcolumn reaction with ninhydrin. Prior to analysis, the samples were hydrolyzed in 6 M HCl in sealed and evacuated tubes at 110 °C for 24 h.

2.9. Surface Coatings. For cell-attachment analyses, polystyrene or glass surfaces were coated with the AK-cyclo[RGDfC] or with one of the control peptides (PLL, AK, AK-cyclo[RADfC], AK-RGDfC). The peptides were dissolved in distilled water in concentrations of 0.002−20 μg/mL. The solutions were left on the surfaces for 30 min, then aspirated, and the surfaces were allowed to dry at room temperature. Estimated surface densities—pretending that all molecules were deposited to the surface—were calculated between 0.00025 and 2.5 $\mu g/cm^2$. Coated surfaces could be stored for up to 4 months at 4 °C.

2.10. Atomic Force Microscopy. The morphology of the AK-cyclo[RGDfC] polypeptide layer after drying for at least 24 h was studied with an atomic force microscope (Park Syst. XE-100, South Korea). We used a cantilever NSC15 (Park Syst.) made of Si_3N_4. The tip curvature radius was less than 10 nm and the reflective side was coated with Al. The AFM scans were conducted at 0.3−0.5 Hz scanning rate taken at scan window of 2 × 2 μm. Several randomly selected locations with at least 8−10 different images were collected for each specimen. Observation was carried out at noncontact mode in air. The image analysis was performed using the XIE 1.6 progam (Park Syst.).

The morphology of the protein layers on the glass substrate was characterized by average roughness values (R_a) determined for the whole images.

2.11. Cell Cultures. Cell lines (MDCK, GENC, A431, A7r5, NE-4C, MC3T3-E1 sc4) and HUVEC cells were maintained

Table 3. Investigated Cell Types

name	cell type	origin	maintaining medium	reference
MDCK (madine darby canine kidney)	cloned kidney epithelial	canine	DMEM, 10% FCS	ATCC No.: CCL-34
GENC (glomerular endothelial cell)	cloned glomerular endothelial	mouse	DMEM, 10% FCS	31
A431	cloned epidermal epithelial	human	DMEM, 10% FCS	ATCC No.: CRL-2592
A7r5	cloned aorta smooth muscle	rat	DMEM, 10% FCS	ATCC No.: CRL-1444
NE-4C	cloned neuroepithelial stem cell	mouse	MEM, 4 mM glutamine, 5% FCS	32
MC3T3-E1 sc4	cloned osteoblast	mouse	αMEM, 10% FCS	ATCC No.: CRL-2593
HUVEC (human umbilical vein endothelial cell)	umbilical endothelial	human	M199, 15% FCS	ATCC No.: CRL-1730
primary neurons	neuron	mouse	MEM, 4 mM glutamine, 10% FCS	33
primary astrocytes	astrocyte	mouse	MEM, 10% FCS	34
primary fibroblast	fibroblast	mouse	DMEM, 10% FCS	35
bone marrow mesenchyme	mesenchyme	mouse	DMEM/F12 1/1 (v/v), 10% FCS + 5% HS	36

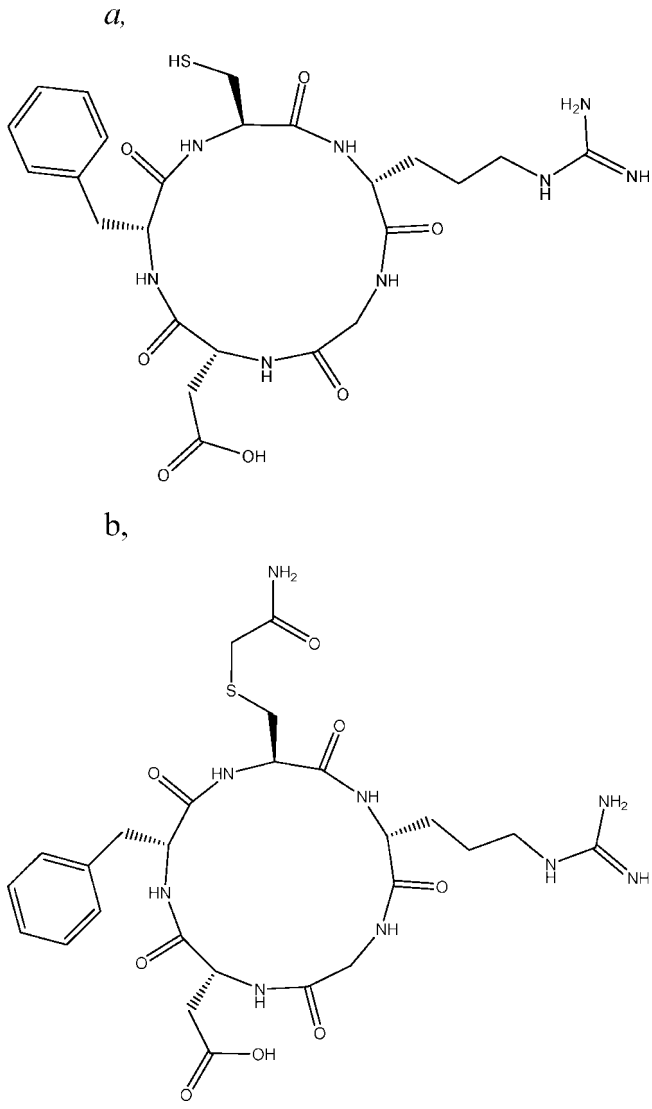

Figure 1. Structure of cyclo[RGDfC] (a) and cyclo[RGDfC(Cmc)] (b).

under standard culture conditions described for the particular cell type (Table 3). Primary cell cultures of neurons (*33*) and astrocytes (*34*) and maintained preparations of fibroblasts (*35*) and bone marrow mesenchymal cells (*36*) were established from mouse tissues and were maintained according to well established protocols, in serum-containing media (Table 3).

For cell-attachment assays, the cells were harvested by trypsinization (0.05 w/v % trypsin, in phosphate buffered saline [PBS] containing 5 mM EDTA). After inhibiting the enzyme activity and washing, the cells were collected in the maintaining media, but without serum. The cells were reseeded onto coated surfaces and were allowed to attach for no longer than 3 h (see below).

For analyzing the 48 h survival, harvested glomerular endothelial cells (GENC) were collected, seeded, and maintained in defined medium composed of DMEM/F12 3/1 (v/v) and supplemented with 1% ITS (ITS-G, GIBCO, Invitrogen) providing a final concentration of 10 μg/mL insulin, 5.5 μg/mL transferrin, and 6.7 ng/mL sodium selenite.

2.12. Microscopic Observations on Initial Cell Adhesion. 35 mm tissue culture dishes precoated with various peptides were placed into a thermo-stabilized (37 °C) chamber on the stand of a Zeiss Axiovert 200 M microscope. 1.5 mL suspensions of cells (5×10^5 cells/mL) in serum-free media were seeded and phase-contrast pictures ($10 \times$ objective) were taken at various time-points after seeding.

Time-lapse microscopic comparison of the initial attachment of MDCK cells on AK- cyclo[RGDfC] and on PLL is available in the Supporting Information. Videomicroscopic analysis was carried out similarly as described above, with a Zeiss Axiovert 200 M microscope. Photographs were taken at every 5 s.

2.13. Quantitative Cell Adhesion Assay. Cells were harvested by trypsinization, centrifuged, and washed with PBS to eliminate trypsin and EDTA and were collected in serum-free media. In some experiments (see the text), the media were supplemented with 5% (v/v) FCS. Cells were seeded into 96-well plates at densities of $(1-5) \times 10^4$ cells/well and were allowed to attach for a time-point, when the majority of cells ($\geq$75%) had adopted a spread-out, flattened shape on AK-cyclo[RGDfC] (1−3 h, depending on the cell type). Cultures were washed with PBS to eliminate nonattached cells and then fixed with 4% paraformaldehyde (w/v in PBS) for 20 min at room temperature. Attached cells were stained with 0.25% methylene blue, for 30 min (*37*). Stained cell mass was dissolved in acidic (0.05 M HCl) ethanol and light absorbance was measured at $\lambda = 650$ nm with a Bio-Rad 450 ELISA reader. For each condition, eight parallel wells were measured. Data were expressed as means and standard deviations.

2.14. Cell Viability Assay. Viability of GENC cells cultured in defined medium was determined by measuring reductive capacity according to Mosmann et al. (*38*). Briefly, cells were grown for 48 h in 96-well plates coated with different peptides and then treated with 3-(4,5-dimethylthiazol-2-yl)-2,5-diphenyltetrazolium bromide (MTT) for two hours at a final concentration of 250 μg/mL. After a 2 h incubation, cells and formazan crystals were dissolved in acidic (0.08 M HCl) isopropanol. Optical density was determined at a measuring wavelength of $\lambda = 570$ nm against $\lambda = 630$ nm as reference with a Bio-Rad

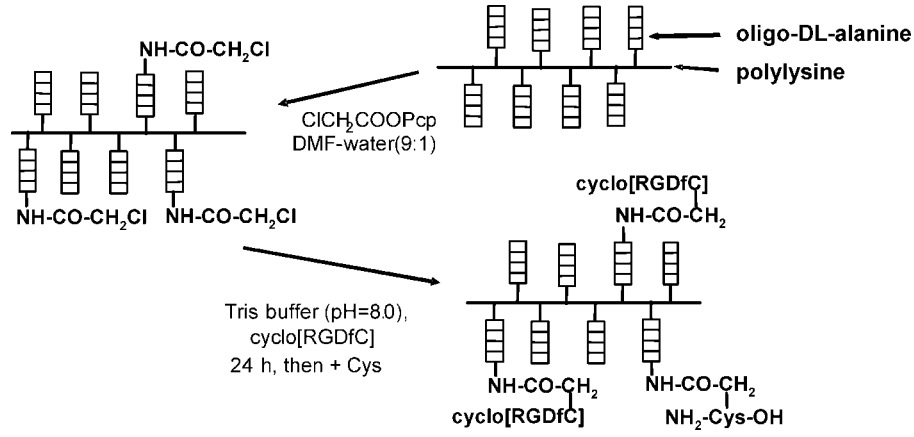

Figure 2. Conjugation of cyclo[Arg-Gly-Asp-D-Phe-Cys] to AK carrier molecule.

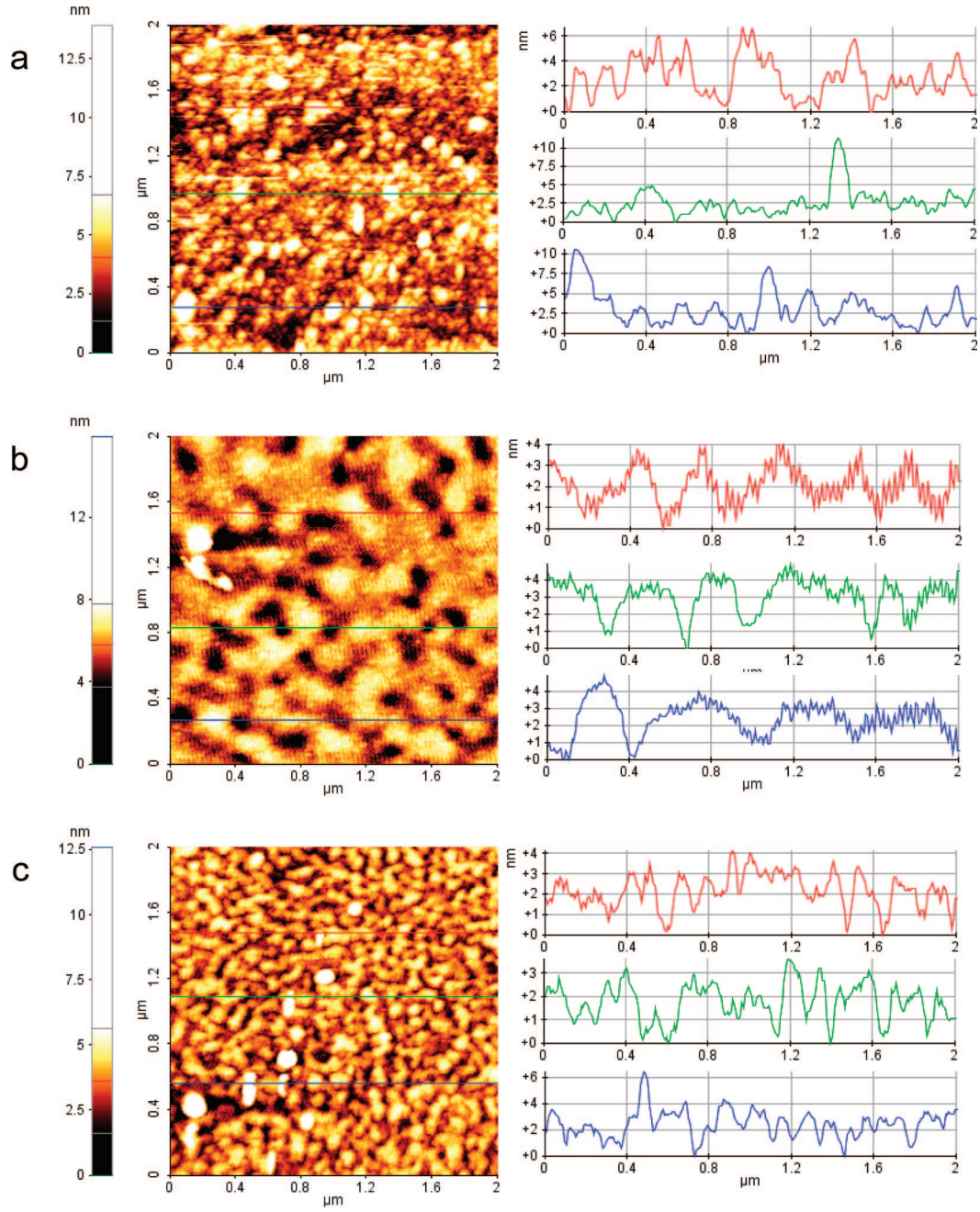

Figure 3. AFM topographic images (2 × 2 μm) of protein films formed from solution with a concentration of 2.5 (a), 0.25 (b), and 0.025 (c) μg/mL. Three selected profile lines are displayed for each image to present typical vertical cross sections of the protein films.

450 ELISA reader. Assays were carried out on 8 parallel wells. The viability data were expressed as means and standard deviations.

2.15. Visualization of Actin Cytoskeleton with Rhodamine-Conjugated Phalloidin. MDCK cells were plated onto AK-cyclo[RGDfC] coated glass coverslips in serum-free medium. They were fixed after 1.5 or 24 h with 4% paraformaldehyde for 20 min. The cell membranes were permeabilized by 5 min treatment with 0.1% Triton-X 100 (in PBS). Actin cytoskeleton was labeled with rhodamine-conjugated phalloidin according to the manufacturer's instruction (Invitrogen) and analyzed with a Zeiss Axiovert 200 M fluorescent microscope.

2.16. Statistical Analysis. All data were expressed as means and standard deviations. Statistical significance was determined by Student's *t* test. Differences were considered significant at $p < 0.05$.

3. RESULTS

3.1. Synthesis and Characterization of Cyclic RGD Conjugated AK Polymer. The aim of the present study was the development of cell adhesive conjugates carrying the biologically active integrin ligand, cyclic RGD peptide (cyclo-[RGDfC]) (Figure 1a) to provide potent adhesive surfaces for a wide range of cell types. As macromolecules with polycationic property bind readily to negatively charged tissue culture dishes and metal oxide surfaces, a polycationic branched polypeptide AK (Figure 2) with polylysine backbone was selected, in which oligo-DL-alanine moieties were introduced as branching side chains (poly[Lys(DL-Ala)$_m$]). The resulting AK (Figure 2) was used as polymeric carrier. The cyclic peptide cyclo[RGDfC] and also its cyclic and linear control derivatives (cyclo[RADfC] and H-RGDfC-NH_2)—which served as control peptides—were coupled to the AK polymer *via* thioether bonds. The thioether

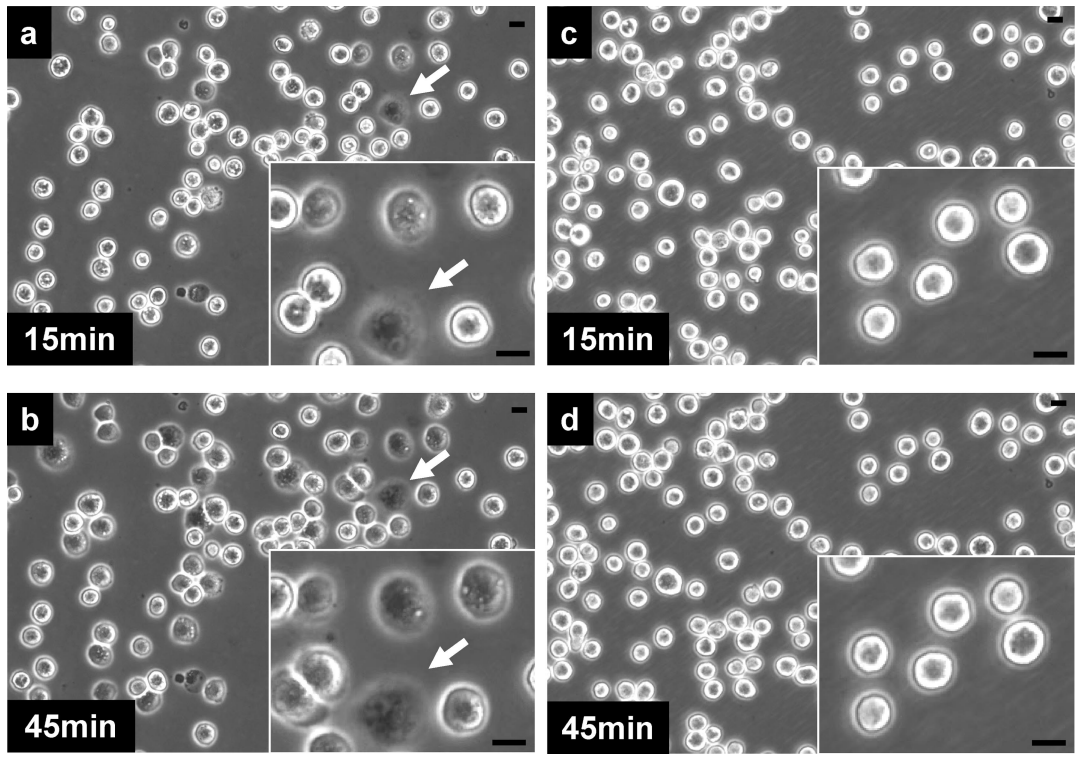

Figure 4. Initial attachment of MDCK cells on AK-cyclo[RGDfC] (a,b) and PLL (c,d) coated plastic surfaces. Pictures were taken at 15 and 45 min after plating. Note spreading cells (arrows) on the enlarged inserts on the left panels. Bars represent 10 μm.

linkage has several advantages such as easy and selective formation and high stability under the conditions of the chemical synthesis, purification, and biological measurements. For the formation of the thioether bond, the AK polymer was chloroacetylated using ClAc-OPcp, and a cysteine residue was incorporated into the sequence of the RGD peptides. To avoid the racemization during the "head-to-tail" cyclization step, glycine or alanine were the C-terminal amino acid residues. In this way, a linear, side chain protected precursor peptide with a sequence of DfCRX (X = Gly or Ala) was built up on solid phase. The peptide was prepared on 2-Cl-trityl chloride resin by Fmoc/^{t}Bu strategy. The side chain protected linear precursor peptide with free N- and C-termini (H-D(O^{t}Bu)fC(Trt)R(Pbf)X-OH) was produced by cleavage using a mixture of DCM/MeOH/AcOH = 8:1:1 (v/v/v). The purity of the crude products was over 90%; therefore, they were applied for cyclization without further purification. The "head-to-tail" cyclization was performed in a diluted DMF solution in the presence of BOP and HOBt coupling reagents and DIEA base to provide slightly alkaline conditions. The side chain protecting groups were removed from the cyclic peptides with a modified Reagent-K cleavage mixture. For a comparative study, a thiol-protected form of the cyclic peptide was also produced by carboxamidation of the Cys side chain (c[RGDfC(Cmc)]) (Figure 1b) using iodoacetamide. In order to analyze the importance of the RGD sequence and the cyclic form of the peptide, two further compounds were prepared (cyclo[RADfC] and H-RGDfC-NH_2) for conjugation. The peptides were characterized by RP-HPLC and ESI-MS (Table 1). Racemization study of cyclo[RADfC] showed no significant epimerization of Ala under cyclization conditions.

Prior to conjugation, the AK polymer was "activated" by chloroacetylation of the amino groups of the polypeptide using ClAc-OPcp at a molar ratio that resulted in about 40% substitution of the side chains of the polymer. The incorporated chlorine atoms could be exchanged for thiol-containing cyclic peptides in a nucleophile substitution reaction under slightly alkaline conditions. To avoid significant dimerization of the cysteine containing cyclic peptides by disulfide bond formation, the cyclic peptides were added in solid form to the solution of the choloracetylated polypeptide and the concentration of the peptide was kept low in the reaction mixture. After the conjugation reaction, unreacted chloroacetyl groups were blocked by the addition of an excess of cysteine to prevent alkylation during the biological experiments. The amount of the attached RGD peptides was calculated by the results of amino acid analysis (Table 2). In all three cases, 32−33% substitution of the branches of the polypeptide carrier was observed.

3.2. Coverage of the Substrate by the Deposited Peptide−Conjugates. Topographic AFM images (Figure 3) on peptide-coated glass substrates showed that the AK-cyclo[RGDfC] polypeptide conjugate formed continuous layers on the substrate. The roughness values of peptide-covered surfaces highly exceeded the values obtained for the pure glass (R_a < 0.1 nm) substrate. The surface roughness increased with the increasing peptide concentrations (0.025−2.5 μg/mL) with the average roughness values of 1.056, 0.777, and 0.729 nm for films prepared from solutions with concentrations of 2.5, 0.25, and 0.025 μg/mL, respectively. Sectional analyses on the structural details showed aggregates extending from the layer. The peak values of emerging aggregates reached about 10 nm on surfaces deposited from 2.5 μg/mL peptide solution.

3.3. Cell Adhesion. The initial attachment, spreading, and short-term (24−48 h) survival of different types of cells (Table 3) were investigated on surfaces coated with AK-[cRGDfC] polymer and were compared to the cell behavior on plastic or glass surfaces coated with control peptides. The cell types involved in the studies included cloned cell lines, long-term maintained tissue-derived cells (HUVEC, mouse bone marrow mesenchyme cells, and fibroblasts), and primary tissue cells (neurons, astrocytes) directly isolated by tissue dissociation (Table 3). The control substrates included tissue-culture treated polystyrene, poly(L-lysine) (PLL), the poly(L-lysine-alanine) (AK) carrier polypeptide, the AK-cyclo[R*A*DfC] conjugate with

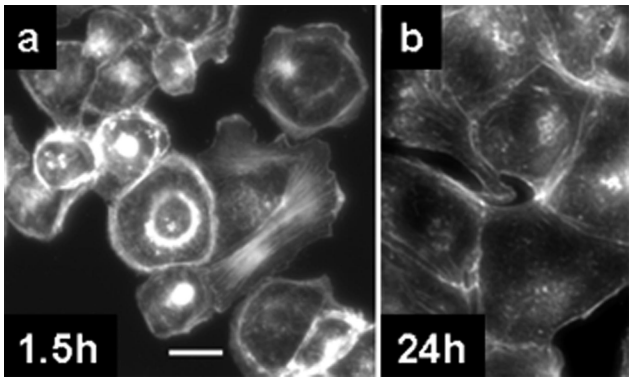

Figure 5. The rearrangement of actin fibers in MDCK cells attaching to (a) and spreading on (b) AK-cyclo[RGDfC] coated glass surfaces were visualized by rhodamine-conjugated phalloidin staining. Pictures were taken 1.5 (a) and 24 h (b) after plating. Bars represent 10 μm.

a corrupted RGD motive, and the AK-RGDfC conjugate containing the linear form of the pentapeptide. Cell attachment was assayed in serum-free environment.

The morphological observations on the cell shape during initial attachment and spreading followed with videomicroscopy (see Supporting Information) and conventional microscopy (Figure 4) indicated a rapid initial attachment to AK-cyclo-[RGDfC] coated surfaces. In the initiation of flattening, however, cell type dependent differences were observed. MDCK, GENC, or NE-4C cells were flattening against the AK-cyclo[RGDfC] coated surface within 10−15 min (Figure 4a), while spreading of MC 3T3 osteoblasts, HUVECs, or astroglial cells was observed no sooner than 40−60 min after plating. In comparison to control surfaces (bare polystyrene, PLL or AK, AK-cyclo[RADfC], AK-RGDfC), however, all cells developed filopodia and lamellipodia earlier on AK-cyclo[RGDfC] and cells flattened in a significantly shorter period (Figure 4).

The rearrangement of actin fibers during attachment to AK-cyclo[RGDfC] was visualized by rhodamine-conjugated phalloidin (Figure 5). In MDCK cells adhering to AK-cyclo[RGDfC] coated surface, spreading cells with actin stress fibers were observed within 1−1.5 h, among cells with an actin arrangement characteristic of initial attachment (*39*), namely, the inner actin ring and the outer actin zone at the actively palpating filopodia (Figure 5a). The cells kept on spreading until settling in a flattened monolayer arrangement (24 h), with stress fibers oriented toward the cell periphery and distributed almost evenly (Figure 5b). The morphological changes indicated that the contact with AK-cyclo[RGDfC] coated surface initiated a normal schedule of attachment, at least as it was judged by the rearrangement of the actin filaments.

Cell attachment was measured by colorimetric cell adhesion assay, modified after Oliver et al. (*37*). Evaluation of the attached cell mass after a period of initial attachment (see Experimental Procedures) revealed that AK-cyclo[RGDfC] promoted the initial attachment of all investigated cells, except freshly isolated neurons.

AK-cyclo[RGDfC] improved attachment if it was deposited from solutions containing 0.025−2.5 μg peptide per cm^2. The sufficient coating density, however, was cell type dependent. MDCK or NE-4C cells needed less dense (0.025 μg/cm^2 or 0.25 μg/cm^2, respectively) coating (Figure 6a), while MC 3T3 osteoblasts, astroglia, or fibroblast cells demanded higher density (2.5 μg/cm^2) for robust attachment (Figure 6b). The adhering cell mass increased with increasing AK-cyclo[RGDfC] density up to an "upper threshold". In the case of MDCK or GENC cells, adhesivity did not increase above the coating density of 0.25 μg/cm^2, while in the case of weakly adhering cells, an "upper threshold" was not reached even at the highest applied (2.5 μg/cm^2) density (Figure 6b). With changing concentration of AK-cyclo[RGDfC] solution, e.g., increasing the density of the coating molecules at the surface, the optimum coats for particular cells could be determined. Addition of fetal bovine serum (5%) to the medium could improve the attachment at low AK-cyclo[RGDfC] surface densities in the initial (1.5−3 h) period, but failed to influence cell attachment at or above the optimum coating density (Figure 7).

To test the specific adhesive effects of the cyclo[RGDfC] containing polymer, two different control motifs—a linear pentapeptide RGDfC and a cyclic pentapeptide (cyclo[RADfC])

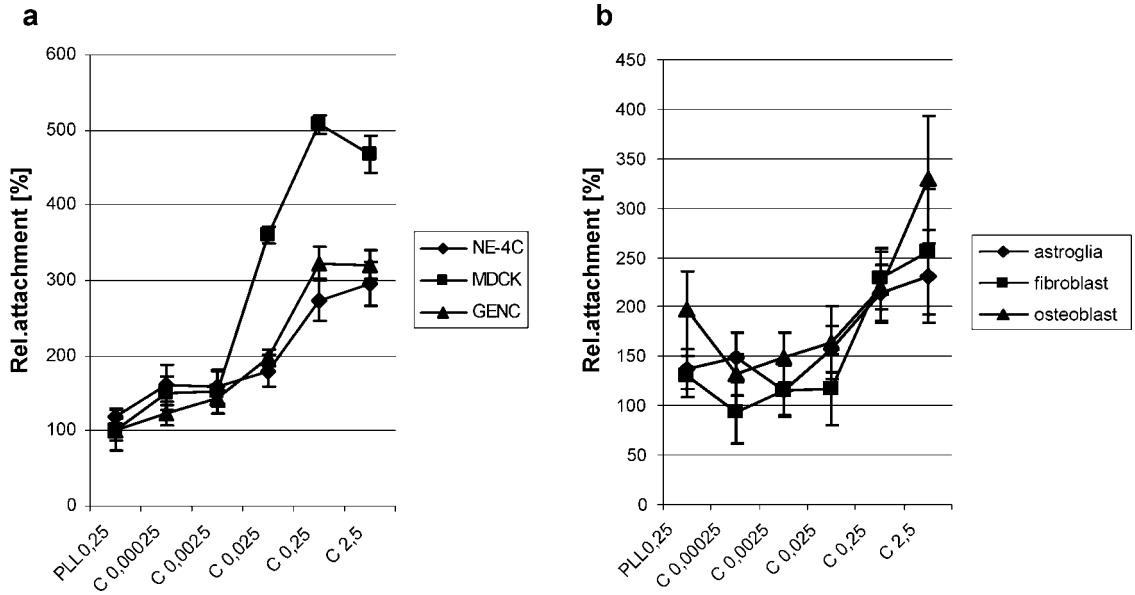

Figure 6. The attachment of different types of cells to AK-cyclo[RGDfC] deposited from coating solutions containing 0.00025−2.5 μg peptide−conjugate/cm^2. Attachment was determined by photometric evaluation of methylene-blue staining after washing off the unattached cells. The data are presented as the percentages of attachment on polystyrene (100%). Note the cell type dependent differences in the "threshold coating density" for attachment. Attachment of MDCK, GENC, and NE-4C cells (a); attachment of astrocytes, fibroblasts, and osteoblasts (b). (Abbreviations: PLL, poly(L-lysine); C, AK-cyclo[RGDfC]; the numbers indicate the peptide content [μg] in the coating solution calculated for 1 cm^2 surface area). Averages and standard deviations were calculated from 8 identical preparations.

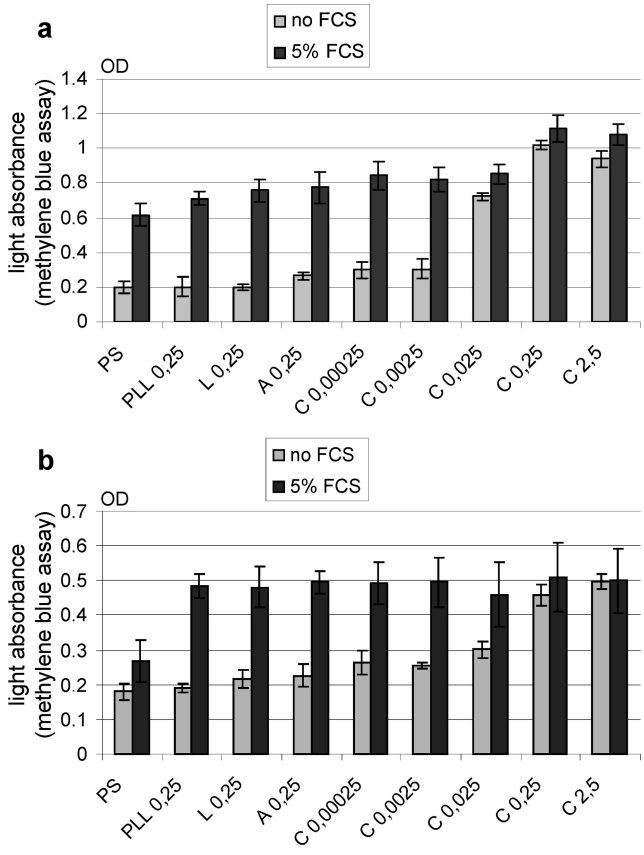

Figure 7. The effect of serum on the attachment of MDCK (a) and NE-4C (b) cells to AK-cyclo[RGDfC], AK-c[RADfC], AK-RGDfC, and poly(L-lysine) coated or bare, tissue culture treated polystyrene surfaces. Attachment was determined by photometric evaluation of methylene blue staining after washing off the unattached cells. The data are shown as averages and standard deviations of optical densities measured in 8 parallel preparations. Note that, above an "upper threshold density" of AK-cyclo[RGDfC], the presence of 5% FCS did not significantly improve the attachment. (Abbreviations: OD, optical density; PS, polystyrene; PLL, poly(L-lysine); A, AK-c[RADfC]; L, AK-RGDfC; C, AK-cyclo[RGDfC]; the numbers represent estimated surface densities of the coating peptides in $\mu g/cm^2$).

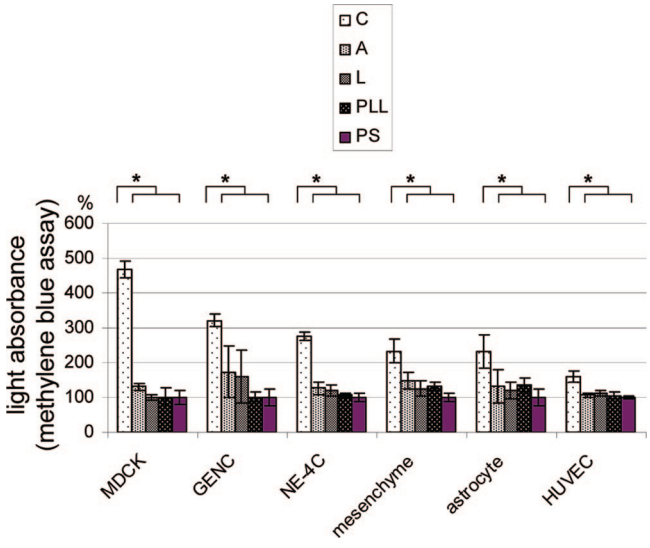

Figure 8. Comparison of initial attachment of various cell types (MDCK, GENC, NE-4C, mesenchyme, astrocyte, and HUVEC) on different substrates. The data are presented as the percentages of attachment on polystyrene (100%). (Abbreviations: PS, polystyrene; PLL, poly(L-lysine); A, AK-c[RADfC; L, AK-RGDfC; C, AK-cyclo[RGDfC]).

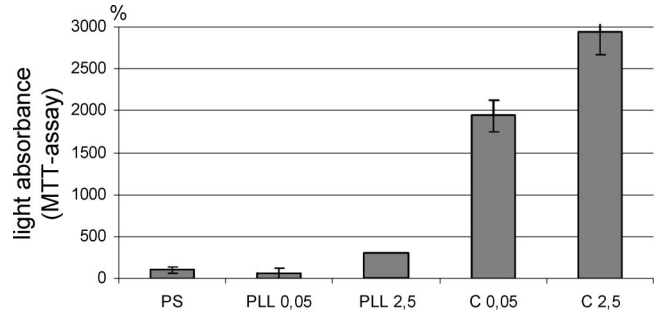

Figure 9. Serum-free survival of glomerular endothelial cells (GENC) on AK-cyclo[RGDfC] coated surfaces. MTT-assay revealed an almost 30-fold increase in viability on AK-cyclo[RGDfC] compared to polystyrene (PS) surface after 48 h. The data are presented as the percentages and standard deviations of viability on polystyrene. (Abbreviations: PS, polystyrene; PLL, poly(L-lysine); C, AK-cyclo-[RGDfC]; numbers represent the estimated surface densities of the coating peptides in $\mu g/cm^2$; 100% represents the OD value of the MTT assay on polystyrene).

with a corrupted RGD-motive—were designed and bound to the AK carrier. Neither the AK-RGDfC nor the AK-cyclo[RADfC] could support the attachment of the investigated cell types (Figure 8). On these substrates, both the morphology of the cells and the rate of attachment were indistinguishable from those observed on PLL or on the pure AK carrier peptide. The data support the importance of the stereochemical structure of the cyclo[RGDfC] motif in mediating cell adhesion.

3.4. Serum-Free Conditions for Growth of Cells. While cell type dependent growth factors have to be provided for long-term culturing of a number of cells, the application of AK-cyclo[RGDfC] surface could prevent anoikis (cell death initiated by lack of adhesion) in the case of anchorage-dependent cells. The AK-cyclo[RGDfC] surface supported a 48 h survival of several (tested for NE-4C, MDCK, GENC) types of cells in defined media (GENC; Figure 9) a "long-term" period if rapid anoikis is regarded. Moreover, serum-free cultures of selected neural stem-like cells were grown on AK-cyclo[RGDfC], in defined media supplemented with epithelial growth factor (EGF), for several weeks (personal communication; Marko et al.; manuscript in preparation). The use of the adhesive peptide conjugate provided strictly defined, serum-free conditions for initiation of cell cultures, and also for long-term growth of selected cell types.

4. DISCUSSION

In the present study, we report on the development of a novel, synthetic cell adhesion polypeptide. The conjugate contains a poly(L-lysine) backbone with oligo-DL-alanine side chains carrying biologically active cyclo[RGDfC] integrin ligand motifs at the N-termini of the oligo-alanine chains. The poly(L-lysine) backbone was chosen for promoting binding to a number of different substrates including tissue culture dishes, glass, and metal oxide surfaces. As was expected, AK-cyclo[RGDfC] bound readily to SiO_2 or metal oxide surfaces as was demonstrated by our previous studies (*40*) using the label-free OWLS technique (*41*).

To increase the accessibility of the attached cyclopeptide, a spacer was built from raceme alanine residues resulting in flexible, unstructured peptide side chains as was confirmed by previous CD analysis on AK polypeptide and related peptides (*42, 43*). The random incorporation of 3 to 5 raceme alanine residues was shown to increase the flexibility of the spacer as well as the solubility of the carrier (*44*). The raceme oligo-alanine side chains increased the steric flexibility of the cyclo[RGDfC] end motif and improved the water solubility of the conjugate by preventing helix formation.

As a biologically active, cell-adhesive moiety, the cyclo-[RGDfC] cyclic pentapeptide was chosen due to the strong affinity of cyclic RGD pentapeptides to cell surface integrins (*19*) and the availability for conjugation through the Cys residue. The introduction of a D-enantiomer phenyalanine into the peptide ring was thought to result in a rigid RGD motif, easily recognized by integrins (*19*). The fact that AK conjugates carrying either the linear RGDfC pentapeptide or the cyclic cyclo[RADfC] peptide (with corrupted integrin binding motif) failed to support cell adhesion suggests that a precise positioning of the RGD sequence plays a crucial role in the enhanced cell-adhesive effect of the cyclo[RGDfC] conjugate. Cyclic RGD-containing peptides were reported to be potent ligands for a series of different integrin receptors, with a predominant selectivity to $\alpha_v\beta_3$, $\alpha_v\beta_5$, and $\alpha_v\beta_6$ (*22*). The specificity of the cyclic pentapeptide for integrin receptors, however, might have been modified as a consequence of coupling to the carrier polymer and also by introducing the Cys amino acid. Our previous observations demonstrated that—at least in the case of the investigated cell types—the soluble cyclo[RGDfC] and cyclo[RGDfV] pentapeptides exerted almost the same effect in cell detachment assays (Marko et al., personal observation).

While the exact amount of molecules for unit areas could not be determined, the density of the RGD-containing motifs on the surface seemed to play a crucial role in adhesivity. We think that with increasing local density of the ligand motifs, integrins displaying lower affinity to the specified ligand will also be implicated in binding, and therefore, the peptide will initiate cell adhesion above a defined "threshold density". Atomic force microscopic studies showed increasing surface roughness and aggregate formation with increasing concentration of the peptide−conjugate in the coating solution. The changing surface topography might contribute to the concentration-dependent adhesion preferences displayed by different cell types.

The AK-cyclo[RGDfC] polymer provided adequate adhesive coating for many different types of cells including cloned cells of epithelial, endothelial, or smooth muscle origin, and tissue-derived astrocytes, fibroblasts, mesenchymal, and neural stem cells.

We found that, below a "threshold" of deposited AK-cyclo[RGDfC], cell adhesion was improved by addition of serum, while at high surface densities of the conjugate, the serum did not affect adhesion. The observation indicates a synergistic action of the AK-cyclo[RGDfC] peptide with some serum components in initial cell adhesion. As fibronectin and vitronectin are the most abundant cell adhesive components in sera (*45*), the findings are in accordance with the notion that cyclic RGD pentapeptides are predominantly fibronectin- and/or vitronectin-mimetic integrin ligands.

As an exception, primary neurons could not adhere to AK-cyclo[RGDfC]. Neurons are known to adhere preferentially to the surface of glial cells or to laminin coatings *in vitro* (*46*), and—in the absence of adequate substrates—they form aggregates. As a consequence and for further application, AK-cyclo[RGDfC] may provide a "panning" surface to sort out non-attaching neurons from readily adhering non-neuronal cells.

For the anchoring of a wide variety of cells, AK-cyclo-[RGDfC] provides a chemically defined adhesive surface coating which supports serum-free cell attachment and survival in the most critical initial period of cell propagation on artificial surfaces. The defined adhesive layer, together with serum-free culture initiation, opens the way for strictly controlled cell cultivation and improves the conditions for growing human cells for therapeutic purposes. Degradation and *in vivo* stability studies should determine whether AK-cyclo[RGDfC] may serve also for coating implant surfaces, especially in cases when rapid attachment of the host cells is required.

ACKNOWLEDGMENT

This work was supported by the Hungarian National Science Fund (OTKA T 049814), Ministry of Health (ETT 202/2006), GVOP-3.2.1.-2004-04-0005/3.0, GVOP-3.2.1-2004-99/3.0., Natl. Science & Devl. Prog. NKFP 1A-060/2004, and NKFP 3A-058/2004. The authors are grateful for Zsuzsanna Környei and Bálint Szabó for their help in videomicroscopy.

Supporting Information Available: Time-lapse microscopic comparison of the attachment of MDCK cells on AK-cyclo-[RGDfC] and PLL substrares. This material is available free of charge via the Internet at http://pubs.acs.org.

LITERATURE CITED

(1) Howe, A. K., Aplin, A. E., and Juliano, R. L. (2002) Anchorage-dependent ERK signaling-mechanisms and consequences. *Curr. Opin. Genet. Devel. 12*, 30–35.
(2) Newman, C. (2003) Serum-free cell culture - the ethical, scientific and economic choice. *Biomed. Sci.* 940–941.
(3) www.focusonalternatives.org.uk.
(4) Bershadsky, A., Chausovsky, A., Becker, E., Lyubimova, A., and Geiger, B. (1996) Involvement of microtubules in the control of adhesion-dependent signal transduction. *Curr. Biol. 6*, 1279–1289.
(5) Hersel, U., Dahmen, C., and Kessler, H. (2003) RGD modified polymers: biomaterials for stimulated cell adhesion and beyond. *Biomaterials 24*, 4385–4415.
(6) Hynes, R. O. (2002) Integrins: bidirectional, allosteric signaling machines. *Cell 110*, 673–687.
(7) ffrench-Constant, C., and Colognato, H. (2004) Integrins: versatile integrators of extracellular signals. *Trends Cell Biol. 14*, 678–686.
(8) Biesalski, M. A., Knaebel, A., Tu, R., and Tirrell, M. (2006) Cell adhesion on a polymerized peptide-amphiphile monolayer. *Biomaterials 27*, 1259–1269.
(9) Comisar, W. A., Kazmers, N. H., Mooney, D. J., and Linderman, J. J. (2007) Engineering RGD nanopatterned hydrogels to control preosteoblast behavior: a combined computational and experimental approach. *Biomaterials 28*, 4409–4417.
(10) Connelly, J. T., Garcia, A. J., and Levenston, M. E. (2007) Inhibition of in vitro chondrogenesis in RGD-modified three-dimensional alginate gels. *Biomaterials 28*, 1071–1083.
(11) Hwang, D. S., Sim, S. B., and Cha, H. J. (2007) Cell adhesion biomaterial based on mussel adhesive protein fused with RGD peptide. *Biomaterials 28*, 4039–4046.
(12) Larsen, C. C., Kligman, F., Kottke-Marchant, K., and Marchant, R. E. (2006) The effect of RGD fluorosurfactant polymer modification of ePTFE on endothelial cell adhesion, growth, and function. *Biomaterials 27*, 4846–4855.
(13) Schuler, M., Owen, G. R., Hamilton, D. W., de Wild, M., Textor, M., Brunette, D. M., and Tosatti, S. G. (2006) Biomimetic modification of titanium dental implant model surfaces using the RGDSP-peptide sequence: a cell morphology study. *Biomaterials 27*, 4003–4015.
(14) Storrie, H., Guler, M. O., Abu-Amara, S. N., Volberg, T., Rao, M., Geiger, B., and Stupp, S. I. (2007) Supramolecular crafting of cell adhesion. *Biomaterials 28*, 4608–4618.
(15) Tugulu, S., Silacci, P., Stergiopulos, N., and Klok, H. A. (2007) RGD-Functionalized polymer brushes as substrates for the integrin specific adhesion of human umbilical vein endothelial cells. *Biomaterials 28*, 2536–2546.
(16) Weber, L. M., Hayda, K. N., Haskins, K., and Anseth, K. S. (2007) The effects of cell-matrix interactions on encapsulated beta-cell function within hydrogels functionalized with matrix-derived adhesive peptides. *Biomaterials 28*, 3004–3011.
(17) Pierschbacher, M. D., and Ruoslahti, E. (1984) Cell attachment activity of fibronectin can be duplicated by small synthetic fragments of the molecule. *Nature 309*, 30–33.

(18) Pierschbacher, M. D., and Ruoslahti, E. (1987) Influence of stereochemistry of the sequence Arg-Gly-Asp-Xaa on binding specificity in cell adhesion. *J. Biol. Chem. 262*, 17294–17298.
(19) Aumailley, M., Gurrath, M., Muller, G., Calvete, J., Timpl, R., and Kessler, H. (1991) Arg-Gly-Asp constrained within cyclic pentapeptides. Strong and selective inhibitors of cell adhesion to vitronectin and laminin fragment P1. *FEBS Lett. 291*, 50–54.
(20) Pfaff, M., Tangemann, K., Muller, B., Gurrath, M., Muller, G., Kessler, H., Timpl, R., and Engel, J. (1994) Selective recognition of cyclic RGD peptides of NMR defined conformation by alpha IIb beta 3, alpha V beta 3, and alpha 5 beta 1 integrins. *J. Biol. Chem. 269*, 20233–20238.
(21) Haubner, R., Gratias, R., Diefenbach, B., Goodman, S. L., Jonczyk, L., and Kessler, H. (1996) Structural and functional aspects of RGD-containing cyclic pentapeptides as highly potent and selective integrin alphaV beta3 antagonists. *J. Am. Chem. Soc. 118*, 7461–7472.
(22) Goodman, S. L., Holzemann, G., Sulyok, G. A., and Kessler, H. (2002) Nanomolar small molecule inhibitors for alphav(beta)6, alphav(beta)5, and alphav(beta)3 integrins. *J. Med. Chem. 45*, 1045–1051.
(23) Barlos, K., Chatzi, O., Gatos, D., and Stavropoulos, G. (1991) 2-Chlorotrityl chloride resin. Studies on anchoring of Fmoc-amino acids and peptide cleavage. *Int. J. Pept. Protein Res. 37*, 513–520.
(24) Gude, M., Ryf, M., and White, P. D. (2002) An accurate method for the quantitation of Fmoc-derivatized solid phase supports. *LIPS 9*, 203–206.
(25) Kaiser, E., Colescott, R. L., Bossinger, C. D., and Cook, P. I. (1970) Color test for detection of free terminal amino groups in the solid-phase synthesis of peptides. *Anal. Biochem. 34*, 595–598.
(26) Szokan, G., Mezo, G., and Hudecz, F. (1988) Application of Marfey's reagent in racemization studies of amino acids and peptides. *J. Chromatogr. 444*, 115–122.
(27) Marfey, P. (1984) Determination of D-amino acids. II. Use of a bifunctional reagent, 1,5-difluoro-2,4-dinitrobenzene. *Carlsberg Res. Commun. 49*, 591–596.
(28) Hudecz, F. (1995) Design of synthetic branched-chain polypeptides as carriers for bioactive molecules. *Anti-cancer Drugs 6*, 171–193.
(29) Mezo, G., de Oliveira, E., Krikorian, D., Feijlbrief, M., Jakab, A., Tsikaris, V., Sakarellos, C., Welling-Wester, S., Andreu, D., and Hudecz, F. (2003) Synthesis and comparison of antibody recognition of conjugates containing herpes simplex virus type 1 glycoprotein D epitope VII. *Bioconjugate Chem. 14*, 1260–1269.
(30) Schoniger, W. (1955) Eine mikroanalytische schnellbesimmung von halogenen in organischen substanzen. *Microchim. Acta 1*, 123–129.
(31) Akis, N., and Madaio, M. P. (2004) Isolation, culture, and characterization of endothelial cells from mouse glomeruli. *Kidney Int. 65*, 2223–2227.
(32) Schlett, K., and Madarasz, E. (1997) Retinoic acid induced neural differentiation in a neuroectodermal cell line immortalized by p53 deficiency. *J. Neurosci. Res. 47*, 405–415.
(33) Madarász, E., Kiss, J., and Bartók, I. (1984) Cell production and morphological pattern formation in primary brain cell cultures. I. Pattern formation within the basal layer(s). *Brain Res. 304*, 339–349.
(34) Környei, Z., Szlávik, V., Szabó, B., Gócza, E., Czirók, A., and Madarász, E. (2005) Humoral and contact interactions in astroglia/stem cell co-cultures in the course of glia-induced neurogenesis. *Glia 49*, 430–444.
(35) Nagy, A., Gertsenstein, M., Vintersten, K., and Behringer, R. (2003) Preparing Mouse Embryo Fibroblast. In *Manipulating the mouse embryo: a laboratory manual* (Nagy, A., Vintersten, K., and Behringer, R., Eds.) pp 371−373, Cold Spring Harbor Press, Cold Spring Harbor.
(36) Urbán, V. S., Kiss, J., Kovács, J., Gócza, E., Vas, V., Monostori, É., and Uher, F. (2008) Mesenchymal stem cells cooperate with bone marrow cells in therapy of diabetes. *Stem Cells 26* (1), 244–253.
(37) Oliver, M. H., Harrison, N. K., Bishop, J. E., Cole, P. J., and Laurent, G. J. (1989) A rapid and convenient assay for counting cells cultured in microwell plates: application for assessment of growth factors. *J. Cell Sci. 92*, 513–518.
(38) Mosmann, T. (1983) Rapid colorimetric assay for cellular growth and survival: application to proliferation and cytotoxicity assays. *J. Immunol. Methods 65*, 55–63.
(39) Defilippi, P., Olivo, C., Venturino, M., Dolce, L., Silengo, L., and Tarone, G. (1999) Actin cytoskeleton organization in response to integrin-mediated adhesion. *Microsc. Res. Technique 47*, 67–78.
(40) Madarász, E., Lefkovets, I., Erdélyi, K., and Szendro, I. (2006) Label-free OWLS assays on the kinetics of cell-attachment: quantification of cell adhesivity. *Progress on post-genome technologies - Proceeding of the 4th International Forum of Post-genome Technologies*, 7
(41) Vörös, J., Ramsden, J. J., Csúcs, G., Szendro, I., De Paul, S. M., Textor, M., and Spencer, N. D. (2002) Optical grating coupler biosensors. *Biomaterials 23*, 3699–3710.
(42) Votavova, H., Hudecz, F., Kajtár, J., Szekerke, M., Sponar, J., and Blaha, K. (1980) Conformation of branched polypeptides based on poly(L-lysine) - Circular-dichroism study. *Collect. Czech. Chem. Commun. 45*, 941–949.
(43) Mezo, G., Hudecz, F., Kajtár, J., and Szekerke, M. (1990) Synthesis and chiroptical properties of model peptides suitable for the immunological characterization of branched polypeptides with the general formula poly[Lys(Xi-DL-Alam)]. *Acta Chim. Hung. 127*, 803–812.
(44) Szokan, G., Mezo, G., Hudecz, F., Majer, Z., Schön, I., Nyeki, O., Szirtes, T., and Dölling, R. (1989) Racemization analysis of peptides and amino acid derivatives by chromatography with pre-column derivatization. *J. Liquid Chromatogr. 12*, 2855–2875.
(45) Underwood, P. A., Bean, P. A., Mitchell, S. M., and Whitelock, J. M. (2001) Specific affinity depletion of cell adhesion molecules and growth factors from serum. *J. Immunol. Methods 247*, 217–224.
(46) Ventimiglia, R., and Lindsay, R. M. (1998) Rat striatal neurons in low-density, serum-free culture, in *Culturing nerve cells*, 2nd ed. (Banker, G., and Goslin, K., Eds.) pp 371−393, MIT Press, Cambridge, Massachusetts.

BC8000134